Enzymatic Degradation of Blends of Poly(ε-caprolactone) and Poly(styrene-*co*-acrylonitrile) by *Pseudomonas* Lipase

KILWON CHO, JAEYOUNG LEE, PEXIANG XING

Department of Chemical Engineering and Polymer Research Institute, Division of Electrical and Computer Engineering, School of Environmental Engineering, Pohang University of Science and Technology, Pohang 790-784, Korea

Received 7 March 2001; accepted 26 May 2001

ABSTRACT: In polymer blends, the composition and microcrystalline structure of the blend near surfaces can be markedly different from the bulk properties. In this study, the enzymatic degradation of poly(ε-caprolactone) (PCL) and its blends with poly(styrene-*co*-acrylonitrile) (SAN) was conducted in a phosphate buffer solution containing *Pseudomonas* lipase, and the degradation behavior was correlated with the surface properties and crystalline microstructure of the blends. The enzymatic degradation preferentially took place at the amorphous part of PCL film. The melt-quenched PCL film with low crystallinity and small lamellar thickness showed a higher degradation rate compared with isothermally crystallized (at 36, 40, and 44°C) PCL films. Also, there was a vast difference in the enzymatic degradation behavior of pure PCL and PCL/SAN blends. The pure PCL showed 100% weight loss in a very short time (i.e., 72 h), whereas the PCL/SAN blend containing just 1% SAN showed ~50% weight loss and the degradation ceased, and the blend containing 40% SAN showed almost no weight loss. These results suggest that as degradation proceeds, the nondegradable SAN content increases at the surface of PCL/SAN films and prevents the lipase from attacking the biodegradable PCL chains. This phenomenon was observed even for a very high PCL content in the blend samples. In the blend with low PCL content, the inaccessibility of the amorphous interphase with high SAN content prevented the attack of lipase on the lamellae of PCL. © 2002 John Wiley & Sons, Inc. J Appl Polym Sci 83: 868–879, 2002

Key words: enzymatic degradation; biodegradation; blend; poly(ε-caprolactone); poly(styrene-*co*-acrylonitrile); surface property

INTRODUCTION

A biodegradable polymer can be degraded into low molecular weight compounds because of the action of micro- and/or macro-organisms or enzymes. The application of biodegradable polymers in the field of solving plastic waste problems and biomedical areas has been widely reported.

Poly(ε-caprolactone) (PCL) is a biodegradable polyester that has been proved to be biodegradable by microorganisms[1] and enzymes.[2] PCL has also proved to be a biocompatible[3] and nontoxic polyester, like poly(glycolic acid) and poly(lactic acid). Early in the 1970s, it was shown that PCL is easily biodegraded and utilized as carbon source by various microbial species.[4,5] The effect of the crystallinity and morphology of PCL on the enzymatic degradation of its films has been studied by Huang and his co-workers.[6–8] They have shown that the degradation takes place first at amorphous regions, prior to the degradation of

Correspondence to: K. Cho (kwcho@postech.ac.kr).

Journal of Applied Polymer Science, Vol. 83, 868–879 (2002)

the crystalline regions. Mochizhuki et al.[9] reported the effects of the draw ratio on the enzymatic degradation of PCL fibers by *Rhizopus arrhizus* lipase. Their results have shown that the enzyme preferentially attacks amorphous or less ordered regions rather than crystalline or more ordered regions of PCL fiber.

The degradation behavior of biodegradable polymers can be controlled by blending them with other miscible polymers. There are a few reports on the biodegradation of miscible blends. These studies include two approaches. In one approach, the blends are composed of two biodegradable polymers, such as a blend of poly(β-hydroxybutyrate) (PHB) and poly(lactic acid) (PLA).[10] In this case, the biodegradation rate and the biodegradation behavior can be controlled by changing the composition of the blend. In the other approach, the blends are composed of one biodegradable and one nonbiodegradable polymer. In regard to the latter approach, Doi et al. reported that there is no weight loss in the miscible blends of PHB and poly(vinyl acetate) (PVAc) when PVAc is major component.[11] When PHB in a PHB/PVAc (74/26 w/w) blend is degraded at the surface layer of this blend, it degrades until only nondegradable PVAc is accessible to the enzymes. For the miscible blends of PHB/cellulose acetate butyrate (CAB),[12] where CAB is a nondegradable polymer, pure PHB is rapidly degraded in the activated sludge, whereas the PHB/CAB blends over the whole composition range (PHB content $<$80%) show no weight loss after 1 year of exposure in activated sludge. At a low PHB content (0–50%), neither weight loss nor erosion is observed because the PHB molecules intimately mixed with CAB molecules at the molecular level are not accessible to microorganisms.[13] Even a PHB-rich blend is not biodegradable because the nonbiodegradable CAB molecules inhibit the access of the enzyme molecules to the pure PHB lamellae. Similar experimental results from the work on the enzymatic biodegradation of miscible blends of PLA/PVAc were also reported.[14] The rate of biodegradation of a PLA/PVAc 95/5 blend is much slower than that of the pure PLA, which is because of the vast difference in the surface tension of pure PLA and the 95/5 blend.

Poly(styrene-*co*-acrylonitrile) (SAN) is a known nonbiodegradable polymer, and PCL is miscible with SAN on a molecular level within a miscibility window of copolymer content ranging from 8 to 28 wt % acrylonitrile in SAN.[15–19] Inside the miscibility window, a one-phase system is formed above the melting point (T_m) of PCL and the glass transition temperature (T_g) of SAN. Below the T_m of PCL, phase separation takes place, and a neat crystalline PCL phase and a homogeneous, amorphous mixture of PCL and SAN exists. Because the microcrystalline morphology and the surface properties of PCL/SAN blends can be controlled easily by the alteration of cooling conditions or blend composition, we chose biodegradable PCL and its miscible blends with SAN to study their enzymatic degradation behavior and reveal its relation with their crystalline microstructure and surface properties.

EXPERIMENTAL

Materials and Sample Preparation

Poly(ε-caprolactone) (PCL), with molecular weight of 80,000, was purchased from Aldrich Corp. Poly(styrene-*co*-acrylonitrile) (SAN), with 24 mol % acrylonitrile (AN) content and a molecular weight 75,000, was received from Cheil Industries Inc. (Korea). The enzyme *Pseudomonas* lipase (PS; 30 units/mg) was purchased from Sigma Corp.

The blends of PCL and SAN were prepared by solution casting using dichloromethane as a solvent. A dilute solution (5% w/w) was stirred continuously for 24 h at room temperature. Then, the solution was cast into glass dishes, dried at room temperature for 3 days, and then dried in a vacuum at 50°C for another 3 days. Solution-blended PCL/SAN thin films were prepared for biodegradation testing by compression molding, and isothermally crystallized at different temperatures (36, 40, and 44°C for pure PCL, and 40°C for PCL/SAN blends) for 48 h. The thickness of the films was /0.1 mm. The PCL/SAN films contained 1, 3, 5, 10, 20, 40, and 60% SAN.

Thin films for the polarized optical microscopic observation were prepared by solution casting and subsequent melt crystallization. Three drops of the dilute solution were first put on a clean glass slide, then the slide kept for 3 days at room temperature, and held for another 3 days in a vacuum at 50°C. After drying, the remaining films were melted at 80°C in an oven for 24 h, then they were isothermally crystallized at selected temperatures for 48 h at a hot stage in another oven.

Enzymatic Degradation

The enzymatic degradation of PCL and its blends was carried out in a 0.025 M phosphate buffer

solution (pH = 7.0) containing PS at 0.5 mg/mL at 37 °C. The film samples were each 10 ×10 mm^2 in size and ~ 10 mg in weight. The samples and solution were incubated in a test tube and were shaken in a water bath. After a determined period of time, the films were picked out and washed with distilled water, and then dried in a vacuum at 40°C to a constant weight.

Measurements

The thermal behavior of PCL, SAN, and blends was characterized by differential scanning calorimetry (DSC), with a Perkin Elmer DSC-7 at a scanning rate of 20°C/min. Polarized optical microscopic observation was carried out in a Zeiss Axioplan Microscope at room temperature. The thin films of samples were isothermally crystallized at selected temperatures for the morphological studies.

The contact angle measurements were performed on a contact-angle meter (Kyowa Kaimenkagaku Company, Ltd., Japan) using an environmental chamber at 25°C. The two liquids used for the measurements were water and diiodomethane. The surface tension of the samples was calculated by using a geometric-mean method.[20] The surfaces of the sample films were observed with a scanning electron microscope (SEM, Hitachi S-570). The transection of polymer films was prepared by breaking the film in liquid nitrogen, then coating it with a thin layer of gold-palladium. Small-angle X-ray scattering analyses (SAXS) of films were carried out at room temperature using a Philips PW1700 X-ray diffractometer in the 2θ range 0.1–3.0° at a scan rate of 0.05°/min, with a wavelength 0.154 nm (Cu, Kα).

The X-ray photoelectron spectroscopy (XPS) spectra were acquired with an ESCA200i (VG instrument) electron spectrometer employing monochromated Al K-α X-rays. The electron takeoff angle to the spectrometer was 90° from the sample surface, and the irradiated angle of the X-rays was 30° from the sample surface. Survey spectra were collected using a pass energy of 100eV and a step energy 1eV. Narrow scans of the elemental core lines were taken with a pass energy of 50eV and a step energy of 0.05eV.

RESULTS AND DISCUSSION

Crystalline Morphology and Structure of PCL and PCL/SAN Blends

To study the effect of the physical properties and morphology on the enzymatic biodegradation of PCL films, four PCL films with different thermal history were prepared. The semicrystalline polymers showed different crystalline structure for every different thermal treatment. Pure PCL was crystallized at different temperatures (36, 40, and 44°C) after melt compression molding, and one sample was quenched in liquid nitrogen after melt compression, then stored at room temperature for 2 weeks. The morphology and thermal properties of PCL films were determined by polarized optical microscopy, SAXS, and DSC. The polarized optical microscopy study showed that there was no obvious difference in the spherulite structure and size for PCL crystallized at 36, 40, and 44°C, as shown in a representative polarized optical micrograph of PCL crystallized at 40°C (Fig. 1a). But for melt–quenched PCL film, no obvious spherulites were observed (Fig. 1b). The DSC results (Table I) show that the melting temperature of melt crystallized PCL (at 36, 40 and 44°C) was similar, whereas the melt-quenched PCL film shows lower melting temperature and crystallinity.

There are many reports on the miscibility and morphology of PCL and SAN blends.[15–19,21] It was reported that PCL and SAN can form a miscible blend when the acrylonitrile content in the SAN copolymer is 8–28%.[15–19] In our study, acrylonitrile content in the SAN copolymer was 24%, so the blends of PCL and SAN studied here were miscible at all compositions in the melt state. The homogenous phase was observed for the melt film of PCL/SAN under the optical microscope without cross-polarizer, which also indicated that these blends were miscible in the melt state.

PCL/SAN blends isothermally crystallized at 40°C showed that the melting temperature decreased with the increase of SAN content, and their crystallinity normalized by PCL weight percent also decreased drastically when the SAN content was >40% (Table II). The polarized optical microscopy results showed that the spherulite morphology of PCL in the isothermally crystallized blends appeared different from that of the pure PCL when the SAN was added to PCL(Figs. 1c and 1d). The spherulite of pure PCL exhibited only a maltese cross pattern (Fig. 1a), but the PCL/SAN blends with SAN content <20% showed not only a maltese cross, but also distinct extinction rings (Figs. 1c and 1d) that are named 'ring-banded spherulites'.[22,23] Even when only 1% SAN was added to PCL, the spherulite also showed a typical ring-banded texture (Fig. 1c). Li et al.[22] have reported that the rejection of SAN with high

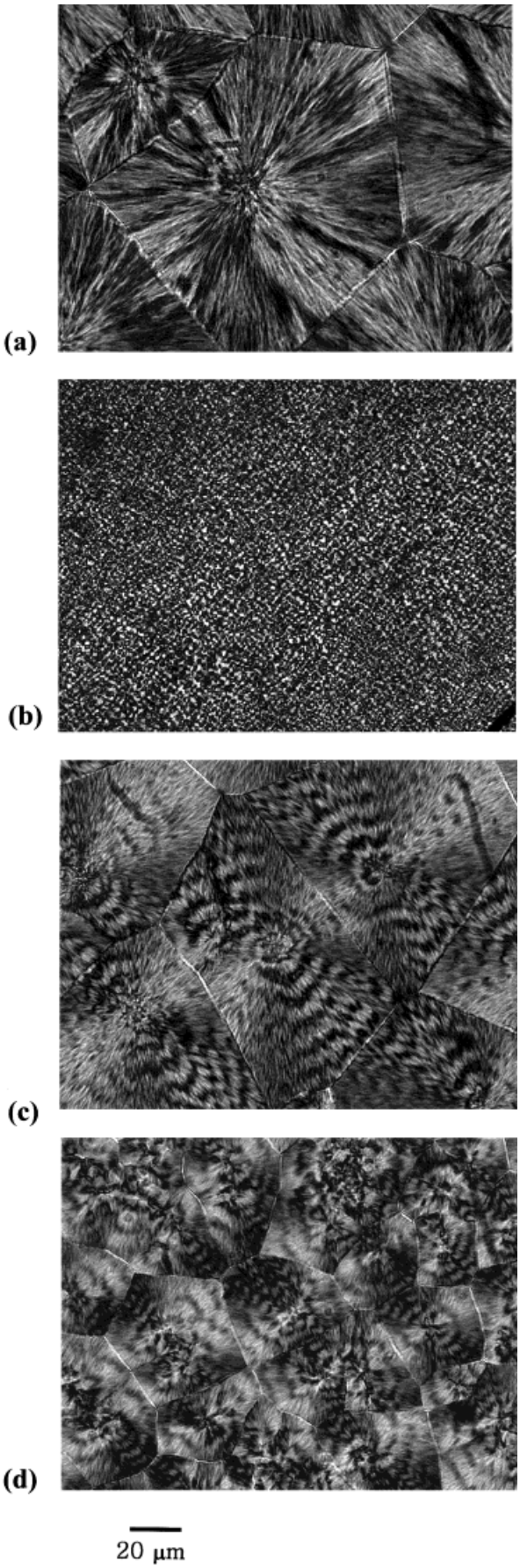

T_g from the lamellae to an interlamellar amorphous region will give rise to stress on the lamellar surfaces and result in twisted lamellae during crystallization,[23] which is the origin of the ring-banded spherulite.

In addition to, the PCL and PCL/SAN blends were characterized using SAXS to monitor the lamellar structure. The long period was estimated using Lorentz-corrected scattering intensities as a function of the scattering vector.[24] The peak maximum from the Lorentz-corrected intensities was employed to compute long periods by Bragg's law. Lamellar thickness was estimated from the scattering data with a one-dimensional correlation function according to the pseudo-two-phase model.[27,28] The long period and lamellar thickness are presented in Tables I and II.

The long period of melt crystallized PCL at 36, 40, and 44°C was quite similar (~ 18.8 nm), whereas that of melt-quenched PCL was 14.8 nm; this result is in agreement with the research of others[25] and lower than the long periods of melt crystallized PCL (Table I). For PCL/SAN blends, when SAN content was <10% in the blends, the values for the long periods were similar (Table II). When the SAN content was >20% in the blends, the long period increased. This kind of increase in the lamellar periodicity of crystallizable PCL in the PCL/SAN blends can be attributed to interlamellar segregation of the noncrystallizable SAN.[26] This result suggests that during the crystallization of PCL from one-phase melt, the amorphous SAN is being rejected from the lamellae into the interlamellar region of PCL, where it forms a homogeneous mixture with the amorphous part of PCL molecules. The lamellar thicknesses obtained for melt crystallized PCL were almost same, whereas the melt-quenched PCL showed lower values (Table I). For PCL/SAN blends, the lamellar thicknesses were quite similar to that of pure PCL (Table II).

Surface Properties

The enzymatic degradation process is a kind of surface erosion phenomenon. Because the surface composition of the polymer is very critical in enzymatic degradation behavior, the surface compo-

Figure 1 Polarized optical micrographs of pure PCL and blends crystallized at 40°C: (a) pure PCL, (b) melt-quenched PCL, (c) PCLSAN1, (d) PCLSAN10.

Table I Thermal Properties and Solid Structure of PCL with Different Thermal Histories

Sample	Cryst. Temp (°C)	Time (h)	T_m (°C)	ΔH_m (J/g)	Crystallinity (%)[a]	L_p (nm)[b]	l_c (nm)[c]
PCL40	40	48	56.9	63.8	46.9	19.0	5.7
PCL44	44	48	57.6	63.2	46.5	17.7	5.3
PCL36	36	48	57.0	66.2	48.7	18.3	5.8
PCLQ[d]	melt-quenched		52.4	58.0	42.7	14.8	4.3

[a] Bulk crystallinity from DSC.
[b] The long period was estimated from the Lorentz-corrected SAXS intensities as a function of scattering vector for pure PCL samples.
[c] Lamellar thickness was estimated from the one-dimensional correlation function according to the pseudo-two-phase model.
[d] The sample was first quenched in liquid nitrogen after melting, then stored for 2 weeks at room temperature (~ 25°C).

sition of PCL/SAN blends was determined from the XPS data; that is, the quantity of electrons emitted from the 1s orbitals of carbon, oxygen, and nitrogen atoms of PCL/SAN blends was determined.[29] A comparison of the experimentally determined surface SAN concentration with the bulk weight percent of SAN in PCL/SAN blends is plotted in Figure 2. If the surface composition was identical to the bulk composition, one would expect a linear relationship like as straight line in Figure 2. However, the results in Figure 2 shows that the surface weight percent of SAN is not directly proportional to the bulk weight percent of SAN, and the surface weight percent of SAN is larger than that of the bulk at low content of SAN. This result indicates that there was an excess of the SAN molecules at the surface of the blend.

The surface composition of the blend is generally different from the bulk composition. The important factors in the determination of surface composition for a blend are known to be polydispersity, crystallinity, and the surface energy of the individual polymer.[30] In this case, the surface energy of PCL was nearly similar to that of SAN, as shown in Table III. Therefore, the main reason for the enrichment of SAN at the surface of the PCL/SAN blends might be attributed to the difference in the crystallinity of each polymer: PCL is a crystalline polymer (crystallinity: 50%), whereas SAN is an amorphous polymer. Because amorphous SAN molecules are not able to crystallize in the PCL/SAN blends, the concentrations of SAN molecules at the surface tend to be higher than in the bulk for PCL/SAN blends.

Enzymatic Degradation of Pure PCL Films

It is reported that PCL can be easily degraded by enzymes, such as PS[31,32] and *Rhizopus arrhizus* lipase.[33,34] The effects of molecular weight, crystallinity, and morphology on the microbial and enzymatic degradation of PCL films have been

Table II Thermal Properties and Solid Structure of PCL and PCL/SAN Blends

Sample	T_m (°C)	ΔH_m (J/g)	Crystallinity (blend) (%)[a]	Crystallinity (PCL) (%)	L_p (nm)[b]	l_c (nm)[c]
PCL40	56.9	63.8	46.9	46.9	19.0	5.7
PCLSAN1	57.6	63.2	46.5	48.1	17.7	5.5
PCLSAN3	56.2	64.8	47.6	48.5	17.7	5.5
PCLSAN5	56.8	65.3	48.0	50.5	17.7	5.5
PCLSAN10	56.6	61.3	45.0	50.0	18.3	5.6
PCLSAN20	56.3	53.8	39.5	49.4	20.4	—
PCLSAN40	55.6	39.1	28.8	47.9	23.1	—
PCLSAN60	54.9	18.3	13.4	33.6	—	—

[a] Bulk crystallinity from DSC.
[b] The long period was estimated from the Lorentz-corrected SAXS intensities as a function of scattering vector for PCL/SAN blends samples.
[c] Lamellar thickness was estimated from the one-dimensional correlation function according to the pseudo-two-phase model.

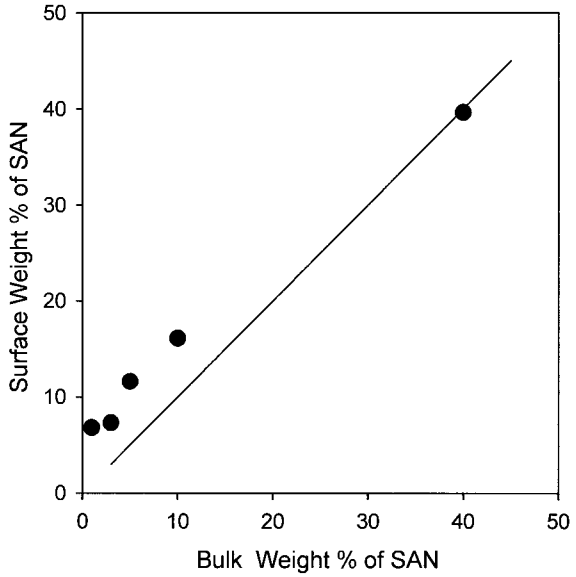

Figure 2 Surface weight percent of SAN against bulk weight percent of SAN for PCL/SAN blends. The surface weight percent of SAN is determined from C, O, N 1s peak of the XPS data. The solid line indicates that the surface composition is identical to the bulk composition.

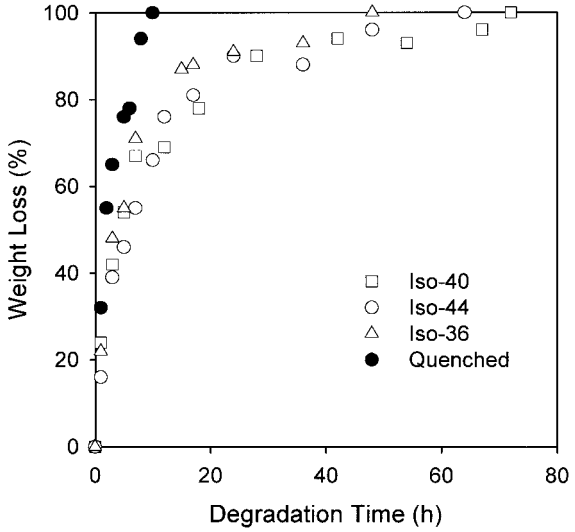

Figure 3 Weight loss percent as a function of degradation time for the enzymatic degradation of pure PCL film.

reported.[7,8] It has been concluded that the degradation proceeds to degrade the amorphous regions prior to degrading crystalline regions. Furthermore, a study on the effects of the draw ratio of PCL fibers on enzymatic degradation[9] has been conducted. It was found that the rate of enzymatic degradation of the fiber is faster at a lower draw ratio than at a higher draw ratio, which may be attributed to less crystallinity in the PCL fiber with a lower draw ratio. In our experiments, the PCL was isothermally crystallized at three temperatures (36, 40, and 44°C), and one sample was crystallized at room temperature after melt quenching in liquid nitrogen. It was found that the rate of enzymatic degradation of the three isothermally crystallized samples was quite similar (Fig. 3) in the experimental condition with 0.5 mg/mL PS.

Table III Results of Surface Energy Analysis

Sample	Surface Energy (dyne/cm^2)
PCL40	43.6
PCLSAN1	44.0
PCLSAN3	43.2
PCLSAN5	44.8
after weight loss 19%	42.0
PCLSAN10	45.3
after weight loss 9%	43.0
PCLSAN20	44.4
PCLSAN40	45.8
PCLSAN60	45.9
SAN	44.5

The SEM photographs of the surface of melt crystallized PCL (at 40°C) before and after enzymatic degradation are shown in Figure 4. Before enzymatic degradation, the surface of PCL film was quite smooth (Fig. 4a). After enzymatic degradation, the surface of PCL film was apparently blemished by the action of PS and the degraded surface became very rough (Figs. 4b and 4c), because the degradation first took place in the amorphous region of the spherulites. At higher magnification (Fig. 4c), the piece and bundle of lamellae are clearly visible, which indicates the enzymatic degradation first took place at the amorphous phase prior to the crystalline part of PCL. The transection of degraded PCL film, shown in Figure 4d, clearly indicates that the enzymatic degradation was a surface erosion phenomenon. The enzymatic degradation proceeded via hydrolysis and dissolution[35] on the surface of films. Even though the enzymatic degradation was a surface erosion phenomenon, DSC also could be used to measure the change of crystallinity of degraded films because the PCL film was very thin (0.1 mm) before degradation. Therefore, DSC analysis was carried out for PCL films before

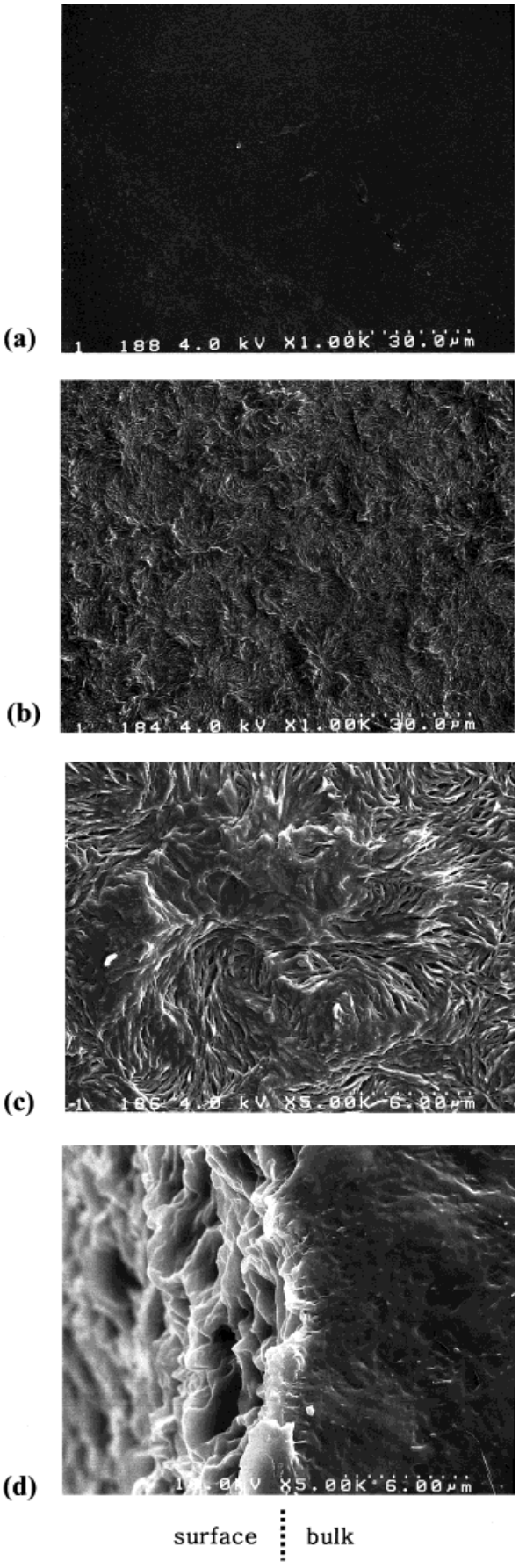

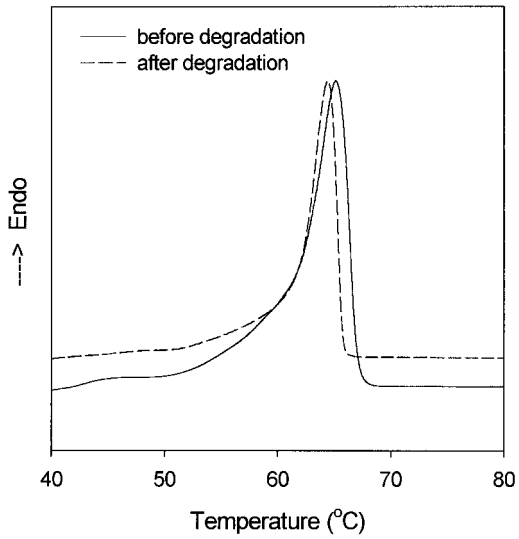

Figure 5 DSC thermograms of PCL films crystallized at 40°C before and after enzymatic degradation for 120 h.

and after degradation (weight loss 85%; Fig. 5), and the crystallinity change is shown in Table IV. The measured results show that the crystallinity of PCL film increased with the degradation above a weight loss of 60%. The crystallinity of PCL film changed from 46.9% (before degradation) to 52.3% (weight loss 85%). This result further supports that the enzymatic degradation preferentially took place in the amorphous part prior to the erosion of the crystalline part[36]

The PS studied here was an endoenzyme that degrades PCL via two stages. The initial stage of enzymatic degradation is a random scission of the ester linkage of the PCL chain in amorphous regions, then further endoenzyme attack on the crystalline regions. Spyros et al.[37] recently reported new evidence, obtained by the proton nuclear magnetic resonance (^{1}H NMR) imaging method, which confirms preferential degradation of amorphous phase of poly(hydroxybutylate) (PHB) and poly(β-hydroxybutyrate-*co*-β-hydroxyvalerate) [P(HB-co-HV)] by PHB depolymerase B from *Pseudomonas lemoignei*. In Figure 5, the degraded PCL film (weight loss 85%) shows a

Figure 4 Scanning electron micrographs of the surfaces of pure PCL films crystallized at 40°C before (a) and after (b, c) enzymatic degradation for 120 h [(c) is the higher magnification of (b)], and (d) is the transection of degraded PCL film broken in liquid nitrogen.

Table IV Crystallinity of PCL with Different Weight Losses after Enzymatic Degradation[a]

Weight Loss (%)	ΔH_m (J/g)	Crystallinity (%)
0	63.8	46.9
35	63.1	46.4
60	69.4	51.1
85	71.1	52.3

[a] The sample was PCL crystallized at 40°C (PCL40).

lower melting temperature than the initial PCL film. A possible explanation is that the PS eroded and broke the PCL chains in the crystalline part, thus reducing the perfection of crystal or the thickness of lamellae after the initial hydrolysis of the chain of the amorphous part of PCL.

The rate of weight loss of melt-quenched PCL is much higher than that of melt-crystallized PCL films. The SEM photograph (Fig. 6) shows the surface of melt-quenched PCL film after degradation. The degraded surface was relatively smooth, which was greatly different from the degraded surface of melt crystallized PCL film (Figs. 4b, c, d). No clear piece or bundle of lamellae was observed, and the surface was not very rough after degradation because of the lack of spherulite. It has been reported that the rate of enzymatic degradation increases with a decrease in crystallinity, spherulite size, and perfection.[38–40] Doi et al. proposed a model that indicates the enzymatic degradation rate of melt-crystallized PHB and its

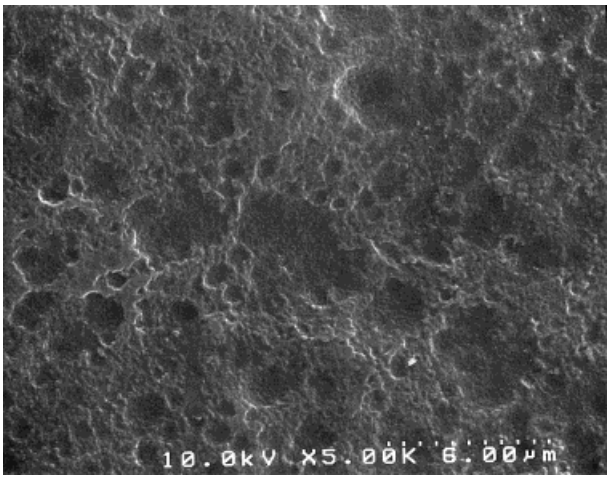

Figure 6 Scanning electron micrographs of the degraded surfaces of melt-quenched PCL films after enzymatic degradation for 120 h.

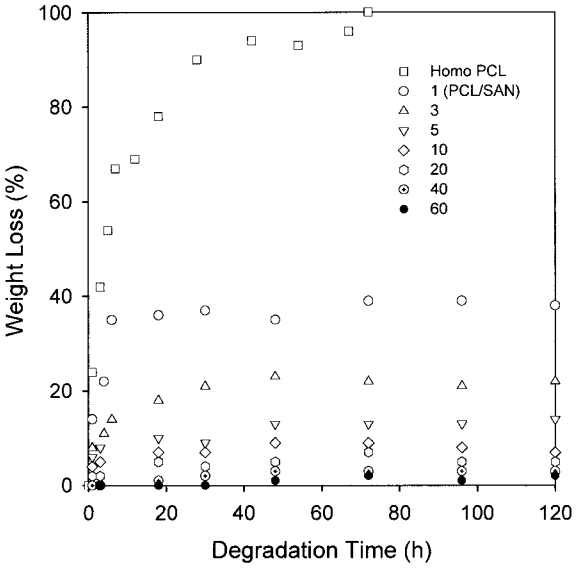

Figure 7 Weight loss percent as a function of degradation time of the enzymatic degradation of PCL/SAN film crystallized at 40°C.

copolyester films increase markedly with a decrease in the lamellar thickness.[41] The PCL films studied in this work showed a greater lamellar thickness (~ 5.74 nm) for melt-crystallized PCL films and less thickness(4.29 nm) for melt-quenched PCL film (Table I). Therefore, the low crystallinity, thinner lamellae, and small size of spherulite (perhaps the size of spherulite is too small to observe under polarized optical microscope) of melt-quenched PCL film may be responsible for its high degradation rate in comparison to that of the melt-crystallized films.

Enzymatic Degradation of PCL/SAN Blends

The weight loss of the enzymatic degradation of PCL/SAN blends as a function of time is shown in Figure 7. It can be clearly seen that the degradation rate for PCL/SAN blends decreased with the increase in SAN content. The weight loss percent reached almost 100% for melt-crystallized (at 40°C) pure PCL film after 72 h of enzymatic degradation. But for PCL/SAN blends, the weight loss percent was very low and the degradation almost ceased after 48 h without further weight loss.

Because enzymatic degradation is the surface erosion phenomenon, the surface composition of the blend immersed in the buffer solution is very important to control the enzymatic degradation behavior. Although the characterization of the

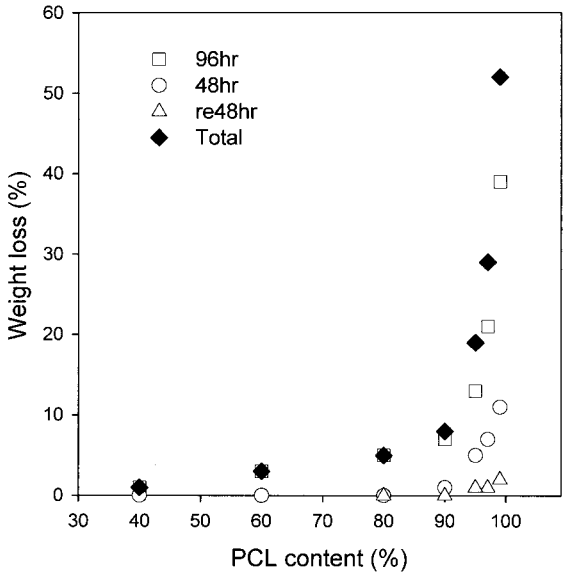

Figure 8 Total weight loss percent of PCL/SAN films (PCL contents are 99, 97, 95, 90, 80, 60, and 40%) after two periods of 48 h of degradation in renewed phosphate buffer solution containing pseudomonas lipase after 96 h of enzymatic degradation.

polymer surface in the air has been well established, there is no direct experimental method of measuring structural changes of the blend surface in the buffer solution. We assume that the surface composition of the blend immersed in the buffer solution is very similar to that in the air due to similar surface energy of PCL and SAN (Table III). Therefore, enzymatic biodegradation behavior can be explained by the surface composition of blend prepared in the air.

The activity of lipase will be decrease after a period of incubated reaction. The absence of weight loss for PCL/SAN blends after 48 h (as shown in Fig. 7), may be due to the inactivity of PS. Therefore, to maintain the activity of lipase during the entire degradation time and to degrade completely the degradable portion of blend films, the blend films degraded for 96 h were further degraded for another 96 h with a new phosphate buffer solution containing fresh PS. After the extended period of 96 h for further degradation, the total weight loss of blend films reached ~ 50, 30, 20, 10, 6, 4, and 2% for PCL/SAN blends with PCL contents of 99, 97, 95, 90, 80, 60, and 40%, respectively (Fig. 8). Especially, during the last period of 48 h, weight loss of blend films was very little (Fig. 8). It is therefore clear that the degradable portion of the blend films was degraded completely by the lipase after another 96 h.

It is interesting that even though 1% SAN was added to PCL, the weight loss only reached ~ 50%. This phenomenon is presumably due to the enrichment of nonbiodegradable SAN molecules at the surface of the film in comparison with the bulk. Although 1 wt % SAN was added to PCL, SAN concentration at the surface was ~ 7 wt % (Fig. 2). Because the enzymatic degradation took place at the surface of the sample, the amount of nonbiodegradable SAN at the surface of the film played an important role in the degradation behavior of the PCL/SAN blend. Therefore, the enrichment of nonbiodegradable SAN molecules at the surface of the film prevented the lipase from effectively attacking the biodegradable PCL chains, and the weight loss of the blend films abruptly decreased to the 50 wt %.

It is known that enzymatic degradation takes place via two steps: the first step is an adsorption of the enzyme on the surface of polymer film, and the second step is a hydrolysis of the polymer chain by the active site of the enzyme.[42] Consequently, the surface energy of film plays an important role in the biodegradation. In this study, the surface energy was determined by a contact angle method using two liquids (water and diiodomethane), and the results are shown in Table III. There was not much difference in the surface free energy of pure PCL, SAN, and blend films before and after biodegradation. Hence, the change of degradation behavior of PCL/SAN blends with SAN content may not be due to the surface energy. This result is somewhat different from other studies done on PLA/PVAc blends. In the biodegradation of PLA/PVAc blends,[14] the low weight loss of PLA/PVAc 95/5 compared with that of pure PLA is due to the change of surface energy from 43.5 dynes/cm for pure PLA to 21.75 dynes/cm for PLA/PVAc 95/5. Therefore, the absorption of the enzyme by the film surface was reduced for PLA/PVAc 95/5 blends compared with that for pure PLA.

The spherulitic morphology was observed in the PCL/SAN blends with PCL content >80% by polarized optical micrographs (Fig. 1). The lamellar thickness determined by SAXS for pure PCL and blends with PCL content >90% was quite similar (Table II). However, comparing Figures 4 and 9, after degradation the SEM photographs of PCL/SAN blends (Fig. 9) show a different surface from the pure PCL (Fig. 4). When the SAN content was 1% the degraded surface was relatively rough. However, for the blends with high SAN content, the degraded surface was relatively

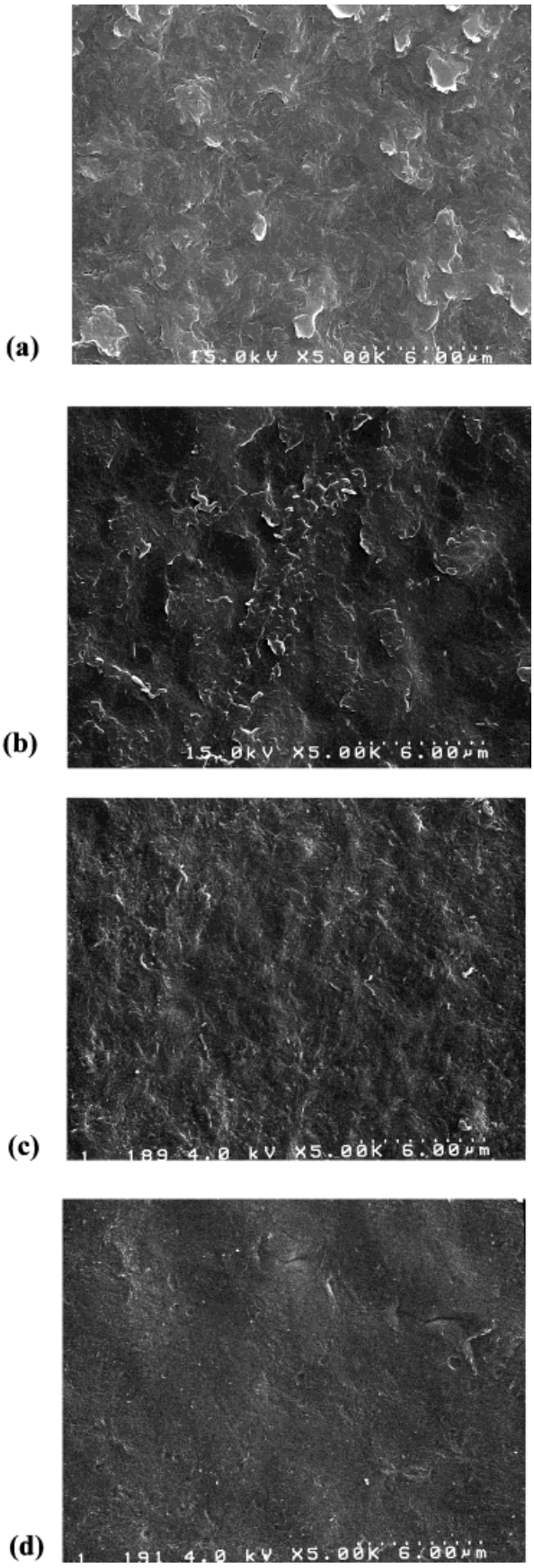

smooth. No obvious piece or bundle of lamellae, like pure PCL, was observed on the surfaces of degraded blend films (Figs. 9c and 9d) even though these blends form spherulite, as can be seen in Figure 1. In this case, the explanations may be divided into two cases depending on the concentration of SAN in the blends.

When the crystallization rate was relatively slow, most of the nondegradable SAN molecules only existed in the amorphous interphase between the lamellae of PCL in melt-crystallized PCL/SAN blends. Therefore, the concentration of SAN in the amorphous interphase may be double its entire concentration in the blends considering the crystallinity of blends (i.e., $\sim$ 40%). As a result, when PCL/SAN blends had a high PCL content (99, 97, 95, and 90%), the concentration of SAN in amorphous interphase was still not very high, which was not very efficient at preventing the lipase attack on the amorphous interphase at the beginning of biodegradation. In this case, the degradable PCL chains were degraded and removed, while the nondegradable SAN chain was still left on the surface. After some degree of degradation the amount of SAN molecular chains on the surface increased to some critical concentration or formed a layer on the surface, which effectively prevented the lipase attack on the PCL molecules, and the degradation ceased. The XPS spectra of the surface of PCL/SAN blend film containing 1 wt % of SAN before and after enzymatic degradation are shown in Figure 10. The results indicate that the N 1s peak due to SAN molecules increased dramatically after 39% weight loss compared with the nondegraded sample. Therefore, XPS results support well the pervious speculation that after degradation, the amount of SAN molecular chains on the surface increases and the degradation ceases.

When the PCL/SAN blends had PCL content of 80, 60, and 40%, SAN concentration in the amorphous interphase was high enough, so the amorphous PCL/SAN interphase was inaccessible to the lipase. In such a case the lipase cannot attack the amorphous interphase and crystalline phase alternately, but can only degrade the PCL crystals on the surface slowly. So the weight loss was very low or almost nonexistent. The schematic

Figure 9 Scanning electron micrographs of the surfaces of PCL/SAN blends films after enzymatic degradation for 120 h: (a) PCLSAN1, (b)PCLSAN3, (c) PCLSAN5, and (d) PCLSAN10.

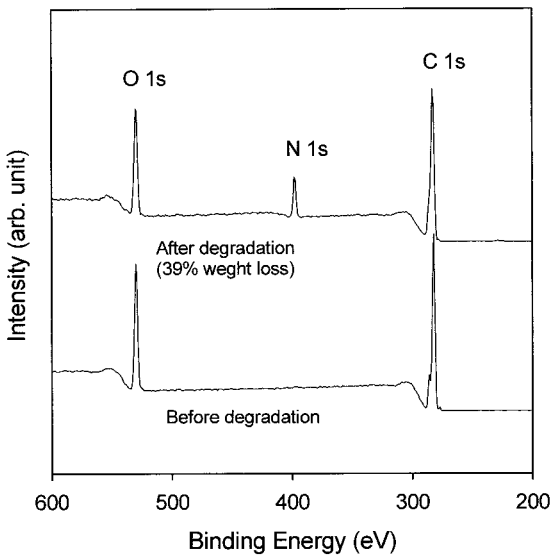

Figure 10 XPS spectra of the surfaces of PCL/SAN blend film containing 1 wt % of SAN before and after enzymatic degradation.

biodegradation pattern for the PCL/SAN blend with different SAN content is shown in Figure 11. A similar result was reported on the biodegradation of PHB/CAB blends.[12] PHB/CAB blends rich in PHB as high as 80% failed to degrade at all after 1 year in the activated sludge, whereas pure PHB completely degraded in 20–25 days. This difference was attributed to the inaccessibility of the amorphous PHB/CAB regions, possibly due to changes in surface hydrophobicity.

CONCLUSIONS

The enzymatic degradation of melt-crystallized films of PCL and its blends with SAN were conducted, and the degradation behavior was correlated with the crystalline micro-morphology and surface composition of the films. Enthalpy measurements and SEM results indicate that the enzymatic degradation in a phosphate buffer solution containing PS preferentially takes place at the amorphous part of PCL film. The melt-quenched PCL film with low crystallinity and small lamellar thickness has a higher degradation rate compared with the isothermally crystallized (at 36, 40, and 44°C) PCL films. The enzymatic degradation studies of melt-crystallized (at 40°C) PCL/SAN films indicate that the pure PCL shows 100% weight loss in 72 h, whereas the blend containing just 1% SAN shows ~ 50% weight loss and degradation ceases, and the blend containing 40% SAN shows almost no weight loss (~ 1%). These results suggest that as the degra-

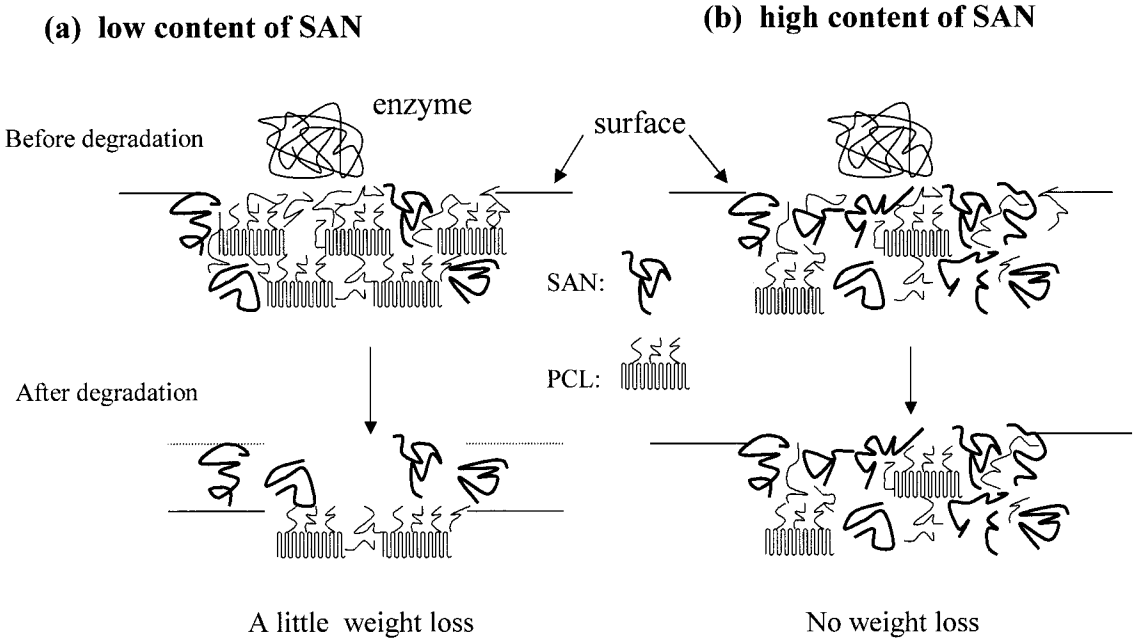

Figure 11 Schematic representation of the biodegradation pattern with the content of SAN at the surface in the PCL/SAN blend: (a) low content of SAN, (b) high content of SAN.

dation proceeds, the nonbiodegradable SAN content increases at the surface of PCL/SAN films and prevents the lipase from attacking the biodegradable PCL chains. In the PCL/SAN blends with low PCL content, the inaccessibility of the amorphous interphase with high SAN content prevents the attack of lipase on the lamellae of PCL. These experimental results suggest that the composition and surface properties, such as crystallinity and its microstructure at the surface, play an important role in the enzymatic degradation of semicrystalline polymers and their blends.

This work was supported by the Ministry of Education of Korea through its BK21 program.

REFERENCES

1. Potts, J. E.; Clending, R. A.; Ackart, W. B. Polym Prepr Am Chem Soc Polym Chem Div 1972, 13, 629.
2. Tokiwa, Y.; Ando, T.; Suzuki, T. J Ferment Technol 1976, 54, 603.
3. Mauduit, J.; Vert, M. STP Pharma Sci 1993, 3, 197.
4. Potts, J. E.; Clendining, R. A.; Ackart, W. B.; Niegisch, W. D. Polym Sci Tech 1973, 3, 1.
5. Tokiwa, Y.; Suzuki, T. R. A. Nature 1977, 270, 76.
6. Cook, W. J.; Cameron, J. A.; Bell, J. P.; Huang, S. J. J Polym Sci Polym Lett Ed 1981, 19, 159.
7. Jar, P.; Huang, S. J.; Bell, J. P.; Cameron, J. A.; Benedict, C. Org Coat Appl Polym Sci Proc 1982, 47, 45.
8. Benedict, C. V.; Cook, V. J.; Jarrett, P.; Cameron, J. A.; Huang, S. J.; Bell, J. P. J Appl Polym Sci 1983, 28, 327.
9. Mochizuki, M.; Hirano, M.; Kanmuri, Y.; Kudo, K.; Tokiwa, Y. J Appl Polym Sci 1995, 55, 289.
10. Koyama, N.; Doi, Y.; Can J Microbiol 1995, 41, 316.
11. Kumagai, Y.; Doi, Y.; Polym Degrad Stab 1992, 36, 24.
12. Tomasi, G.; Scandola, M. J. Macromol Sci Pure Appl Chem 1995, A32, 67.
13. Scandola, M.; Ceccorulli, G.; Pizzoli, M. Macromolecules 1992, 25, 6441.
14. Gajria, A. M.; Dave, V.; Gross, R. A.; McCarthy, S. P. Polymer 1996, 37, 437.
15. Chiu, S. C.; Smith, T. C. J Appl Polym Sci 1984, 29, 178.
16. Nishi, T.; Wang, T. T. Macromolecules 1975, 8, 909.
17. Kressler, J.; Kammer, H. W. Polym Bull 1988, 19, 283.
18. Li, W.; Yan, R.; Jiang, B. J Macromol Sci Phys 1992, B31(2), 227.
19. Li, W. G.; Prud'homme, R. E. J Polym Sci Part B: Polym Phys 1993, 31, 719.
20. Kaelble, D. H. J Adhesion 1970, 2, 50.
21. Kummerlowe, C.; Kammer, H. W. Polym Networks Blends 1995, 5, 31.
22. Li, W.; Yan, R.; Jiang, B. Polymer 1992, 33, 889.
23. Keith, H. D.; Padden, F. J., Jr. Macromolecules 1996, 29, 7776.
24. Vonk, C. G. J Appl Crystallogr 1973, 8, 81.
25. Cheung, Y. W.; Stein, R. S.; Lin, J. S.; Wignall, G. D. Macromolecules 1994, 27, 2520.
26. Oudhuis, A. A.; Thiewes, H. J.; van Hutten, P. F.; ten Brinke, G. Polymer 1994, 35, 3926.
27. Verma, R.; Marand, H.; Hsiao, B. S. Macromolecules 1996, 29, 7767.
28. Talibuddin, S.; Wu, L.; Runt, J.; Lin, J. S. Macromolecules 1996, 29, 7527.
29. Davies, M. C.; Shakesheff, K. M.; Shard, A. G.; Domb, A.; Roberts, C. J.; Tendler, S. J. B.; Williams, P. M. Macromolecules 1996, 29, 2205.
30. Brant, P.; Karim, A.; Douglas, J. F.; Bates, F. S. Macromolecules 1996, 29, 5628.
31. Gan, Z. H.; Liang, Q. Z.; Jing, X. B. Polym Degrad Stab 1997, 56, 209.
32. Wu, C.; Gan, Z. H. Polymer 1998, 39, 4429.
33. Tokiwa, Y.; Suzuki, T.; Takeda, K. Agric Biol Chem 1986, 50,1323.
34. Iwamoto, A.; Tokiwa, Y. J Appl Polym Sci 1994, 52, 1357.
35. Doi, Y.; Kanesawa, Y.; Kunioka, M.; Saito, T. Macromolecules 1990, 23, 26.
36. Cho, K.; Lee, J.; Kwon, K. J Appl Poly Sci 2001, 79, 1025.
37. Spyros, A.; Kimmich, R.; Briese, B. H.; Jendrossek, D. Macromolecules 1997, 30, 8218.
38. Abe, H.; Doi, Y.; Aoki, H.; Akehata, T. Macromolecules 1998, 31, 1791.
39. Kumagai, Y.; Kanesawa, Y.; Doi, Y. Makromol Chem 1992, 193, 53.
40. Koyama, N.; Doi, Y. Macromolecules 1997, 30, 826.
41. Tomosi, G.; Scandola, M.; Briese, B. H.; Jendrossek, D. Macromolecules 1996, 29, 507.
42. Abe, H.; Matsubara, I.; Doi, Y. Macromolecules 1995, 29, 844.